Development of a highly sensitive and selective molecularly imprinted electrochemical sensor for sulfaguanidine detection in honey samples

Nadia El Alami (Last name)El Hassani[a, b] (Last name)

Eduard Llobet[c]

Laura-Madalina Popescu[d]

Mihai Ghita[d]

Benachir Bouchikhi[b]

Nezha El Bari[a, *]

n_elbari@hotmail.com

[a]Biotechnology Agroalimentary and Biomedical Analysis Group, Moulay Ismaïl University, Faculty of Sciences, Biology Department, B.P. 11201, Zitoune, Meknes 50000, Morocco

[b]Sensor Electronic and Instrumentation Group, Moulay Ismaïl University, Faculty of Sciences, Physics Department, B.P. 11201, Zitoune, Meknes 50000, Morocco

[c]MINOS-EMaS, Department of Electronics Engineering, Universitat Rovira i Virgili, Avda. Països Catalans, 26, Tarragona 43007, Spain

[d]Nanostructurated Materials Laboratory, National R&D Institute for Non-Ferrous and Rare Metals, Pantelimon, Ilfov, Romania

*Corresponding author at: B.P. 11201, Zitoune, 50003 Meknes, Morocco.

Abstract

A simple and highly sensitive approach was performed to synthesize a selective sulfaguanidine (SG) sensor based on a molecularly imprinted electropolymer of acrylamide (PAM) for honey quality control. SG was detected by measurements of electrochemical impedance spectroscopy (EIS) and differential pulse voltammetry (DPV). These techniques were applied successfully to determine SG with an excellent selectivity when compared to the results of interfering compounds. Furthermore, unprecedented, ultra-low limits of detection (LOD) and quantification (LOQ) of 0.20 $pg\cdot mL^{-1}$ and 0.67 $pg\cdot mL^{-1}$, respectively according to DPV measurements and 0.17 $pg\cdot mL^{-1}$ and 0.57 $pg\cdot mL^{-1}$ according to EIS measurements. The proposed approach is found to be inexpensive, selective and very sensitive, thanks to the good biocompatibility of SG/PAM composite. The results also showed that this sensor was successfully applied to detect SG residues in honey samples with recoveries between 83.9% and 99.7% and had the potential to be further developed for other multiple analytes detection, thus offering an emerging horizon for bio-sensing applications in honey quality control.

Keywords: Sulfaguanidine; Biomimetic; Food control; Honey; Molecularly imprinted sensor

~~1.~~1 Introduction

Sulfaguanidine (SG) is among the most important sulfonamides used to treat and prevent bacterial infection by inhibiting para-aminobenzoic acid conversion (the essential substrate for the growth of certain bacteria) to tetrahydrofolic acid [1]. In other applications, it is employed as growing helper, prescribed to surmount the challenges of managing animal health and food safety. Their efficiency and accessibility led to overuse, prompting bacterial resistance phenomena coupled with therapeutic incompetence in human medicine [2]. The use of SG in apiculture has been known since 1940 when it was used to prevent and to treat diseases in honeybees, e.g., American foulbrood (AFB) or European foulbrood (EFB) [3]. In the European Union (EU), the treatment of honeybees with antibiotics is banned, and thus honey should be free of antibiotic contamination. Therefore, no maximum residue levels (MRL) have been established. In spite of this legislation, some countries such as Switzerland, UK, and Belgium, have set MRLs for SG ranging from 10 $\mu g\cdot kg^{-1}$ to 50 $\mu g\cdot kg^{-1}$ [4].

The detection of sulfonamide residues at low levels in animal products requires efficient sample preparation steps [5]. For this concern, a series of analytical methods have been implemented for the determination of SG by chromatographic techniques such as liquid chromatography/mass-spectrometry [6,7], high-performance liquid chromatography (HPLC) [8], or fluorometry coupled to chromatographic methods [9,10]. However, other performed

techniques have also been used to detect trace levels of SG, among which, electrochemical analysis [11,12], surface plasmon resonance biosensor [13], DNA-sensors [14], capillary electrophoresis [15], spectrophotometry [16] and enzyme immunoassay [17]. Most of these methods are time-consuming, solvent-usage intensive, expensive and low sensitive, which limit its use in quality control laboratories for SG analysis in pharmaceutical dosage forms.

In our previous work, we have already developed novel electrochemical sensors describing the development of molecularly imprinted polymers (MIPs) and immunosensors for doxycycline [18], sulfapyridine [19], and tetracycline [20] determination in honey samples. The mean advantage of immunochemical techniques lies in the high specificity the antibodies. However, they remain an expensive approach and cannot be reused after their first contact with the target antigen. Consequently, the high cost of these techniques led researchers to create new synthetic materials able to mimic the role of antibodies, and which can selectively recognize a target molecule. One of such approaches consists of using molecular imprint polymers (MIP) since they display some definite advantages over antibodies for biosensor technology, namely, simplicity, stability at the extreme pH and temperature, reusability, low-cost, and simple designing of selective binding sites in polymeric matrices [21]. These characteristics offer great promise for the development of stable artificial bio-sensing elements in environmental monitoring [22], clinical [23], and food analysis [24]. Until today, various MIPs for sulfonamides detection in fish [25], pork [26], chicken [27] and milk [28] samples have been developed, usually as solid-phase extracting sorbents or as the stationary phase for HPLC. Few MIP applications for SG detection have been performed until now. Among them, a molecularly imprinted polymer was already reported for the determination of SG residues in wastewater from the pharmaceutical industry [29], but with a too high limit of detection of about 5 $ng \cdot mL^{-1}$ was reported.

In this paper, we report the development of a new, inexpensive, selective and highly sensitive electrochemical sensor aimed at improving the monitoring of SG in honey at part-per-trillion levels. The sensor developed, which contains recognition sites for SG as a template molecule, was synthesized based on a molecularly imprinted electropolymer of acrylamide. The steps of the surface modification of the developed sensor were investigated by Fourier transform infrared spectroscopy, scanning electron microscopy and energy-dispersive X-ray spectroscopy, as well as electrochemical techniques. This approach based on MIP electrochemical sensor has resulted in an easy synthesis process and a significant enhancement in the detection limit of SG for complex matrices such as honey. More generally, we believe that the present results open up new opportunities to detect other antibiotic contaminants in various food products.

~~2.~~2 Materials and methods

~~2.1.~~2.1 Reagents

Sulfaguanidine (SG), sulfadiazine (SD), sulfamethoxazole (SZ), ethanol (99.8%), phosphate buffered saline (PBS), tetrabutylammonium fluoroborate (TBAFB), acetonitrile, potassium hexacyanoferrate (II) and (III) ($K_4[Fe(CN)_6]$, $K_3[Fe(CN)_6]$) were all purchased from Sigma-Aldrich, France. *N*,*N*-methylenebisacrylamide (NNMBA), acrylamide (AAM) were provided by Honeywell Fluka, Germany. Ultra-pure water was used throughout the experiments. A honey sample assured SG-free was commercially issued from Secrets d'Apiculteur, France.

~~2.2.~~2.2 Apparatus

The Au-SPEs were purchased from Dropsens, Spain (DRP-8X220AT) and had a round working gold electrode of 2.56 mm in diameter, a flat silver material acting as pseudo-reference and a platinum counter electrode. The electrodes were connected to a portable potentiostat PalmSens BV, the Netherlands and the PSTrace 5.2 software was used to connect the device to a measuring computer. The software automatically gathered and stored the outputs of the sensors. The chemical and structural analysis of the modified Au-SPE was conducted by Fourier-transform infrared spectroscopy (FT-IR) technique before and after electropolymerization and extraction steps. This analysis was performed at room temperature via an FT-IR spectrophotometer HATR, ABB, MB3000, Canada. The spectra were carried out for baseline correction, normalization and the resulting spectra peaks at specific wavenumber (cm^{-1}) were analyzed in transmittance mode in a wavenumber range of 500–4000 cm^{-1} with a resolution of 4 cm^{-1}. While, the morphology of electrode surfaces was studied by scanning electronic microscopy (SEM) using QUANTA 250 ~~TM~~™ FEI scanning electron microscope, USA equipped with a GSED detector for secondary-electrons imaging and an energy-dispersive detector for energy-dispersive X-ray spectroscopy (EDX) analysis. SEM images were taken at 20 kV accelerating voltage under a high-vacuum system with a pressure of about 80 Pa.

~~2.3.~~2.3 Preparation of the molecular imprinted polymer (MIP)

The surface of the Au-SPE was cleaned firstly by washing three times with ethanol (99.8%), then with ultra-pure water and dried under nitrogen flow. The MIP membrane is fabricated through the electrochemical polymerization. This step is performed by CV (thirteen cycles) in the potential range from −0.2 V to 0.3 V with a scan rate of 20 $mV \cdot s^{-1}$. The polymerization solutions contain 1 M of acrylamide (AAM) (functional monomer), 0.07 M of *N*,*N*-methylenebisacrylamide (NNMBA) (cross-linking agent), 0.05 M of SG (template), all in acetonitrile medium using tetrabutylammonium fluoroborate (TBAFB, 0.1 M) as the electrolyte. High-purity nitrogen was bubbled at 3 min to remove dissolved oxygen before electro-polymerization. Fig. 1 shows the cyclic voltammograms during the electropolymerization of the monomers indicating that the current gradually decreases with each scan cycle, due to the continuous formation of polyacrylamide (PAM)/SG composite film that obstructs the electron transfer from/to the redox probe of $[Fe(CN)_6]^{3-/4-}$ toward the surface of the gold electrode. In the present case, the AAM electropolymerization in acetonitrile is conducted by a nucleation-and-growth mechanism, which is characterized by cycles with a crossover of the reverse cathodic scan over the anodic scan, giving rise to the so-called “nucleation

loop". Such kind of CV profiles have been interpreted as due to polymer nucleation effects [30]. After that, the template was extracted by washing the film in acetonitrile containing TBAFB (0.1 M) and simultaneously applying a constant potential of 0.4 V for 5 min. The MIP sensor was then, ready to use, after washing thoroughly with distilled water. Similarly, the non-MIP is also fabricated in the absence of SG molecule.

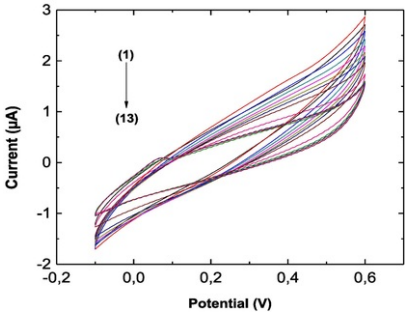

Fig. 1 Process of electro-polymerization of MIP film: thirteen cyclic voltammograms in the potential range from −0.1 V to 0.6 V with a scan rate of 20 $mV \cdot s^{-1}$.

alt-text: Fig. 1

~~2.4.~~2.4 Electrochemical characterization

Cyclic voltammetry (CV), differential pulse voltammetry (DPV) and electrochemical impedance spectroscopy (EIS) measurements were performed at room temperature in a solution of 5.0 mM $[Fe(CN)_6]^{3-/4-}$ prepared in phosphate-buffered saline (PBS) (pH 7.4). The potential range of CV measurements was scanned between −0.4 V and +0.6 V at a scan rate of 30 $mV \cdot s^{-1}$. SG detection was performed by DPV in the potential range from −0.1 V to +0.2 V with a scan rate of 10 $mV \cdot s^{-1}$ and a pulse time of 0.1 s. While the electrochemical impedance spectroscopy was measured in the 0.1 Hz to 50 kHz frequency range with a direct potential (DC) of 0.35 V/ref. and an alternating potential (AC) of 10 mV.

~~2.5.~~2.5 Effect of monomer concentration and template extraction time

The effects of functional monomer concentration in the polymerization process and the time of template extraction on the performance of the MIP sensor were investigated in six distinct devices. The AAM concentration was optimized in the range of 0.1 to 1.0 M for the polymerization process (Fig. 2A). The result indicated that the peak current of oxidation regenerated from CV measurements decreased with the concentration increasing up to 0.7 M and then slightly changed from 0.7 M to 1.0 M. This should be ascribed to the polymer growing on the electrode surface resulting in the film resistance. In this study, 1 M of AAM monomer was selected for obtaining the optimal polymerization signal.

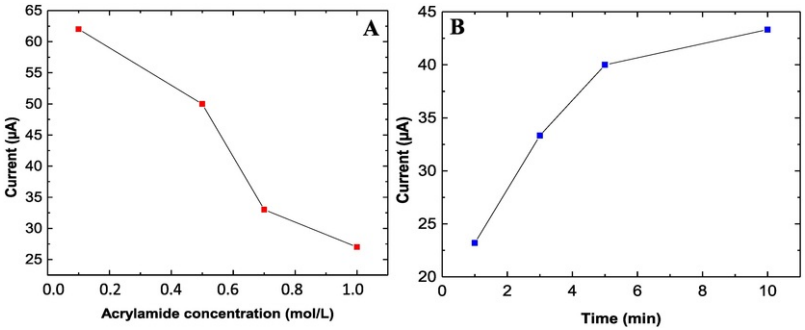

Fig. 2 Optimization of: (A) Acrylamide concentration in polymerization process; (B) Time of constant potential wash of template on the MIP sensor.

alt-text: Fig. 2

For the extraction process, the template molecule was removed by chronoamperometry at 0.4 V in a time interval between 1 min and 5 min (Fig. 2B). The obtained results showed that the peak current of CV measurements increased with the extraction time until 3 min and stabilized from 3 min to 5 min. Consequently, the optimal extraction time in this experiment was set to 5 min.

~~2.6.~~2.6 Selectivity experiment

The selectivity of MIP sensors depends on different factors like the size of the cavities and rebinding interaction. This step was realized by incubating the fabricated SG sensor with three interfering molecules, namely sulfacetamide (SA), sulfadiazine (SD) and sulfamethoxazole (SZ), whose residues are widely found in honey and royal jelly [31].

~~3.~~3 Results and discussion

~~3.1.~~3.1 Preparation of sulfaguanidine imprinted sensor

The polyacrylamide/SG composite resulting from electropolymerization was built upon the gold working area of the SPE (Fig. 3A). The choice of the gold electrodes has been made according to their excellent conductive electrical properties, as well as being biologically inactive, allowing to improve the sensitivity of detection and to increase the electron transfer at the electrode surface. While a judicious choice of the functional monomer is crucial for successful imprinting, which requires strong template binds. In this experiment, we choose AAM as the functional monomer for its low cost and the fact that it can combine with SG to form imine groups, which offer a fast and highly specific attachment. As illustrated in Fig. 3B, the functional monomer and template molecule were allowed to interact before polymerization. The AAM monomer was firstly positioned spatially around SG template leading to a pre-organized approach, which uses reversible covalent bonds between carbonyl groups of AAM and amine groups of SG to give a rather homogeneous population of binding sites and reducing the non-specific connections. Subsequently, the position AAM-SG was fixed by copolymerization with NNMBA as the cross-linking monomer.

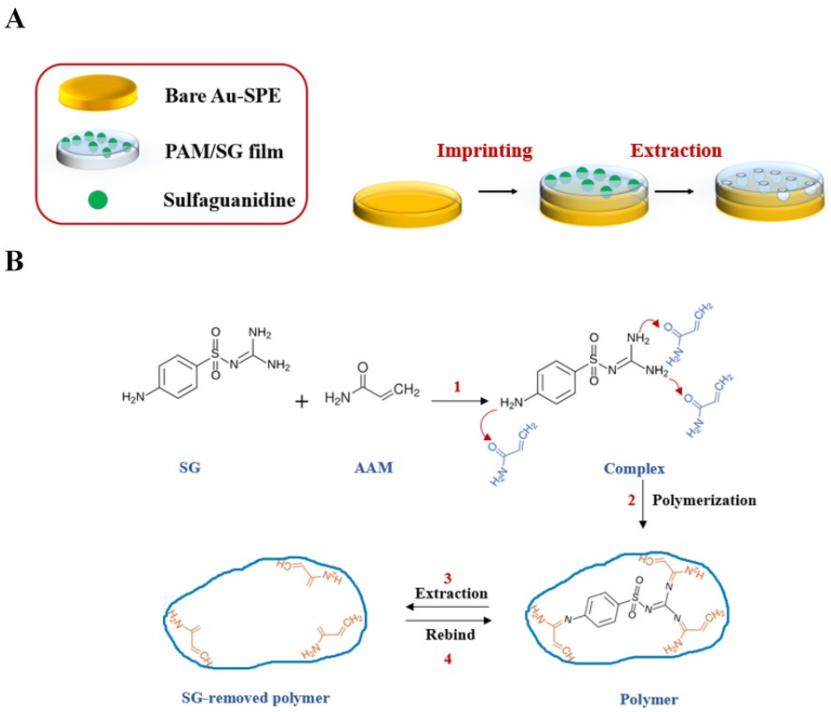

Fig. 3 (A) Steps of MIP preparation sulfaguanidine imprinted polyacrylamide (PAM/SG film), 2: PAM film after template extraction; (B) Chemical scheme of sulfaguanidine imprinting process.

alt-text: Fig. 3

To remove the template from the polymer matrix, it is necessary to cleave the covalent bonds. The binding sites were created by extracting the template molecule by applying a constant potential wash at 0.4 V for 5 min thus facilitating the release of the template because of film swelling. The system sensitivity was studied by preparing an additional SPE with a non-imprinted polymer (NIP) employing the procedure described above, except that the SG-template is not present in the polymerization media.

3.2.3.2 – Morphological and chemical characterizations

The morphology and chemistry of the developed sensor surfaces were examined by scanning FT-IR spectroscopy, SEM microscopy, and EDX analysis. The FT-IR characterization was performed at all steps of Au-SPE surface modifications. Fig. 4 shows the FT-IR spectra collected during sensor preparation process involving measurement of typical absorption profile of bare gold, PAM/SG layer and the subsequent template extraction. The spectrum of gold was included in Fig. 4A in which we notice the relevant information of the gold surface support. While the presence of SG in the polymer matrix was evidenced in Fig. 4B by C=N bonds at 1620 cm^{-1} and 1651 cm^{-1} as found in [32], the substituted benzene ring at 825 cm^{-1} and the symmetric stretching bonds of O=S=O at 1132 cm^{-1} as has already been found by Chandran et al. [33]. However, the –CNS bonds of SG molecules and the secondary amines unattached to the polymeric film were evident at 1520 cm^{-1} and 3362 cm^{-1}, respectively [34]. The amide functions introduced by both monomer and cross-linker have displayed absorption bonds at 3294 cm^{-1} and 968 cm^{-1} assigned to N–H and C–H stretching vibrations, respectively, [33]. However, Fig. 4C represents the FT-IR spectrum of the MIP matrix after SG removal, indicating the absence of all evident absorption bands of template molecules previously described except that of PAM film. Therefore, this microscopic characterization was efficiently adapted to affirm that the SG molecules were successfully incorporated and completely removed from the polymer structure.

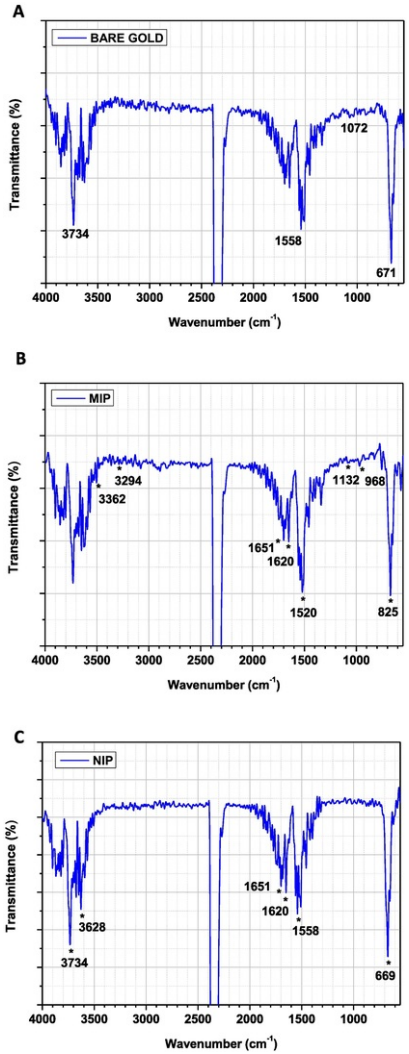

Fig. 4 FTIR spectra of (A) Bare gold; (B) PAM/SG film (MIP); (C) after template extraction (NIP).

alt-text: Fig. 4

Otherwise, the surface morphologies of the electrodes at different modifications were carried out by scanning electron microscopy (SEM) (Fig. 5). As illustrated in this figure, the bare Au-SPE is typically characterized by a rough surface with microporous structure (Fig. 5A). Subsequently, the filling of this microporous structures has been clearly observed in Fig. 5B, indicating the electrode modification with rounded nanostructures of SG embedded in a hydrogel matrix of PAM. Moreover, the template extraction was confirmed by the disappearance of the analyte with the creation of atypical molecular cavities (Fig. 5C). This characterization has indicated that the imprinted sensor is successfully accomplished.

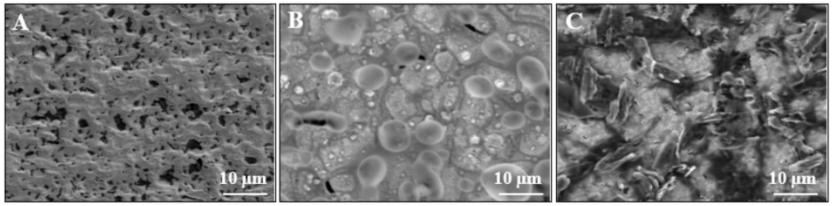

Fig. 5 SEM images of (A) bare gold; (B) PAM/SG layer; (C) MIP sensor after template extraction.

alt-text: Fig. 5

Chemical characterization of electrode surfaces was further performed by Energy-dispersive X-ray spectroscopy (EDX) analysis in order to confirm the finding of the two characterizations above. Fig. 6 illustrates the EDX spectra acquired from the different electrode modifications. Fig. 6A, shows the spectra of bare Au-SPE surface presenting two peaks related to Au and Al atoms from $AuAl_2$ precursor used to fabricate highly porous gold surfaces. The formation of PAM/SG layer was investigated in Fig. 6B. The peaks of S, N, O and C atoms prove the presence of PAM/SG on the electrode surface, while, Cl is attributed to HCl traces used to solubilize SG. After template extraction, we have obtained the EDX spectrum illustrated in Fig. 6C in which we notice a disappearance of the peaks relative to the S and Cl atoms, thus showing the SG extraction from the polymer matrix.

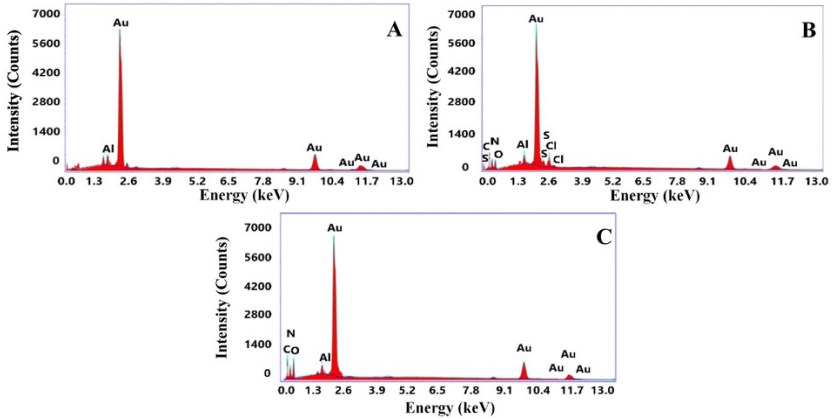

Fig. 6 EDX spectrum of (A) bare gold; (B) PAM/SG modified electrode; (C) MIP sensor after template extraction.

alt-text: Fig. 6

~~3.3.~~3.3 Electrochemical characterization of MIP sensor

To check the fabrication process of the MIP sensor, the changes in the electrode surface were monitored employing EIS and CV approaches, via the assessment of the electrical transfer of the redox system $[Fe(CN)_6]^{3-/4-}$. EIS was chosen as an efficient method to probe the surface-modified electrode and were presented as Nyquist plots in Fig. 7A. The semicircles in high-frequency region imply a controlled charge-transfer process from which the charge transfer resistance (R_{ct}) can be deduced. As one can notice in this figure, bare Au-SPE showed a small-flattened semicircle in comparison to those of functionalized electrodes, which proves that the polymer film modified the surface of bare SPE and highlighted the great enhancement of electrochemical reactivity of the fabricated sensor. After PAM/SG film formation, a high electron transfer resistance was observed indicating the formation of PAM/SG composite film that obstructs the electron transfer from/to the redox probe $[Fe(CN)_6]^{3-/4-}$ toward the surface of the gold electrode, showing that a MIP film is formed on the electrode surface. Cyclic voltammetry assay was also used as a supplementary confirmation technique of the Au-SPE surface modification. The results obtained in Fig. 7B shows the relationship between peak current and the Au-SPE surface modification. This is manifested by the higher separation existing between the peaks of oxidation and reduction potential in comparison to the separation existing between those of bare Au-SPE. This phenomenon proves the increase of charge-transfer resistance as previously identified by EIS characterization.

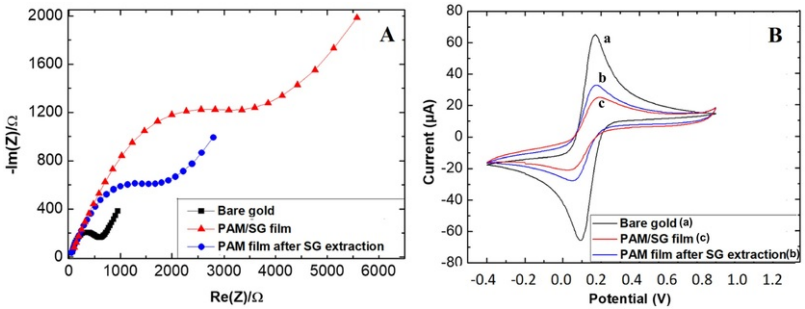

Fig. 7 (A) Nyquist plots of sequential modification steps of Au-SPE toward MIP sensor. Frequency range: from 0.1 Hz to 50 kHz. DC potential: 0.35 V/ref, and AC potential: 10 mV; (B) Cyclic voltammograms of 5 mM $[Fe(CN)_6]^{3-/4-}$ (Scan rate = 50 $mV.s^{-1}$) at Au-SPE electrode after different modification steps of Au-SPE.

alt-text: Fig. 7

~~3.4.~~3.4 Sensor responses

Different concentrations of standard SG solutions were dropped onto the prepared SG-MIP-modified electrodes. DPV and EIS measurements were chosen instead of CV, for the former methods are more sensitive than the latter, allowing the detection of lower SG levels. Differential pulse voltammograms corresponding to different concentrations of SG were recorded and are displayed in Fig. 8A. It can be seen that the increase in SG concentrations induces the decrease of peak values related to the oxidation potential of the electrolyte, which explains the cavity filling by the specific template. To investigate the sensor sensitivity, a non-imprinted polymer (NIP) based device was also prepared. Fig. 8B represents the DPV recorded during the detection of SG with the non-imprinted device. The current intensity of the oxidation peak remains almost unchanged for the different SG concentrations tested, which confirms that the absence of specific cavities able to recognize SG results in the lack of sensitivity of the NIP sensor.

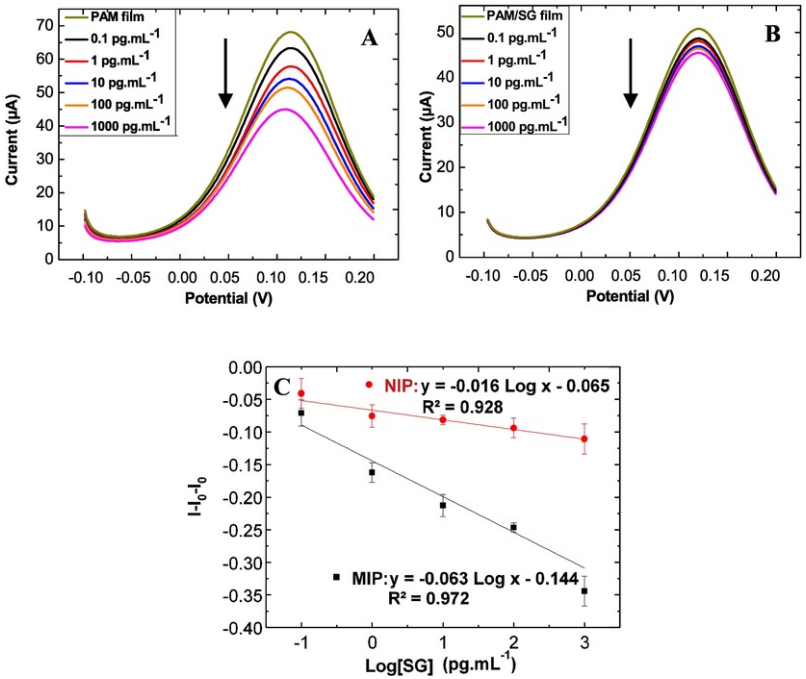

~~Fig. 8.~~Fig. 8 Differential pulse voltammograms obtained after SG detection at different concentrations on (A) MIP; (B) NIP sensors; (C) Calibration curves corresponding to MIP and NIP sensors.

alt-text: Fig. 8

The linear correlation between the peak currents and its corresponding concentrations is illustrated in Fig. 8C by the calibration curves of MIP and NIP sensors as the relative variation of $I-I_0/I_0$ versus logarithmic concentration of SG in a linear range of 0.1 to 1000 $pg.mL^{-1}$. Each point of the calibration curve is the average of three replications. Excellent linearity of both plots was observed with the determination coefficients of 0.972 and 0.928, respectively. Besides, the higher sensitivity of the MIP sensor, expressed by its steeper slope of 0.063 $mL.pg^{-1}$, was observed in comparison to than that of the NIP (0.016 $mL.pg^{-1}$), thus revealing that the electrochemical response did not depend on the non-specific interaction between the polymer and the template.

EIS, as a detection method was carried out to further investigate the sensor, especially to obtain subtle information on the impedance changes during the analyte detection. The quantification of SG at various concentrations is shown in Fig. 9. Herein, the semicircles of Nyquist diagrams correspond to the charge transfer resistance (R_{ct}) after immersing the MIP and NIP sensors in different SG concentrations. Fig. 9A shows the substantial increase in R_{ct} with the increase in analyte concentration, which confirms the successful rebinding of SG into the imprinted cavities. In contrast, the nearly unchanged R_{ct} observed for NIP sensors, reveals the minimal, non-specific interaction existing between the polymer and SG (Fig. 9B). The semi-circular of the Nyquist plot have been excellently fitted with PSTrace 5.2 software using the equivalent circuit shown in the inset of Fig. 9C. The value of $\Delta R/R_0$ was calculated for each SG concentration. The normalized data for the MIP and NIP sensor showed good linearity with the determination coefficients of 0.975 and 0.962, respectively.

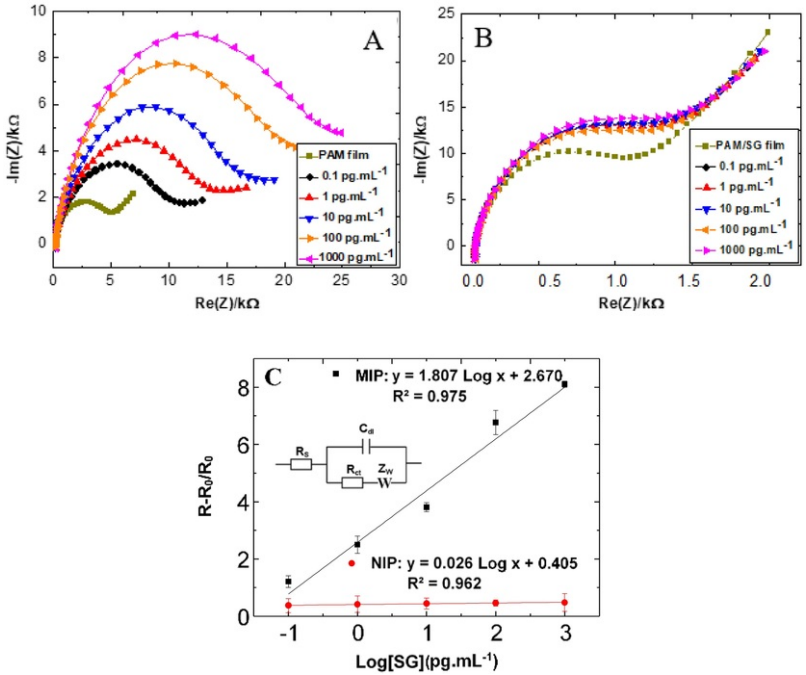

~~Fig. 9.~~**Fig. 9** Nyquist impedance plots in 5 mM of $[Fe(CN)_6]^{3-/4-}$ for SG detection at different concentrations on (A) MIP; (B) NIP sensors. Frequency range: from 0.1 Hz to 50 kHz. DC potential: 0.35 V/ref, and AC potential: 10 mV; (C) The sensitivity of the sensors by normalization o Nyquist plot data. Inset: the equivalent circuit used for EIS fitting, where RS is the solution resistance, Rct is the charge-transfer resistance and Q is the constant phase element.

alt-text: Fig. 9

According to the resulting calibration curves, the slopes of the linear equations are significantly different, which confirm the high sensitivity of the MIP matrix. The limits of detection (LOD) and quantification (LOQ) for this sensor was determined to be respectively 0.20 $pg.mL^{-1}$ and 0.67 $pg.mL^{-1}$ according to DPV measurements and 0.17 $pg.mL^{-1}$ and 0.57 $pg.mL^{-1}$ according to EIS measurements. It is interesting to note that these detection limits of SG are much lower than the MRL from 10 $\mu g.kg^{-1}$ to 50 $\mu g.kg^{-1}$, set in the legislation of Switzerland, UK, and Belgium. A comparison of the LOD and LOQ for the developed MIP sensor and previously published results are listed in Table 1. These results indicate that the developed MIP sensor shows a linear response in a wide concentration range with an extremely low detection and quantification limits.

Table 1 Comparison of various techniques for SG detection.

alt-text: Table 1

Methods	Linear range (ng.mL^{-1})	LOD (ng.mL^{-1})	LOQ (ng.mL^{-1})	Real samples	References
Capillary electrophoresis	1.4–128.5	0.4	1.4	Environmental water	[35]
Liquid chromatography quadrupole-time-of-flight mass spectrometry	15–150	15.0–20.0	–	Milk and fish	[36]
High performance liquid chromatography-tandem mass spectrometry	2.0–150.0	2.0	10.0	Milk	[37]
Enzyme-linked immunosorbent assay	0.2–36.8	2.6	–	Milk	[38]
Molecularly imprinted polymer	0.5–150.0	5.0	10.0	Waste water	[29]
High performance liquid chromatography with fluorescence detection	1.0–100.0	0.2	0.7	Honey	[39]
Light-emitting diode-induced fluorescence coupled to microchip electrophoresis	2.0×10^{3}–1.2×10^{3}	400.0	–	Pharmaceutics and rabbit plasma	[40]
Electrochemical sensor	2.1×10^{3}–4.3×10^{5}	2.1×10^{3}	–	Serum and urine	[11]
MIP sensor	1.0×10^{-4}–1.0	2.0×10^{-4} and 1.7×10^{-4}	6.7×10^{-4} and 5.7×10^{-4}	Honey	This work

~~3.5.~~3.5 Selectivity study

Specific selectivity toward a target molecule is an essential criterion for assessing the performance of any sensor. To estimate the selectivity of the developed sensor, we selected a few molecules with the close chemical structure to SG (Fig. 10) that can coexist in honey samples.

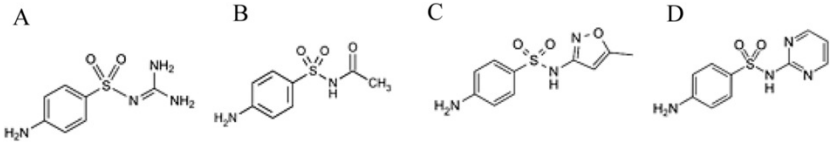

~~Fig. 10.~~Fig. 10 Chemical structure of: (A) Sulfaguanidine; (B) Sulfacetamide; (C) Sulfamethoxazole; (D) Sulfadiazine.

alt-text: Fig. 10

For this purpose, three solutions of sulfacetamide (SA), sulfamethoxazole (SZ), and sulfadiazine (SD) were evaluated as potential interfering molecules. As illustrated in Fig. 11, the interfering molecules had low slopes compared to than that of SG due to their negligible measured changes in current or charge-transfer resistance. Besides, it is clearly observed that the results obtained by EIS measurements in Fig. 11A, shows a high sensitivity to SG compared with those of DPV measurements (Fig. 11B). This finding was explained by the sensitivity of EIS to reveal the slight variation in the chemical structure of the interfering compounds. Therefore, the synthesized MIP based sensor had an excellent recognition specificity for SG.

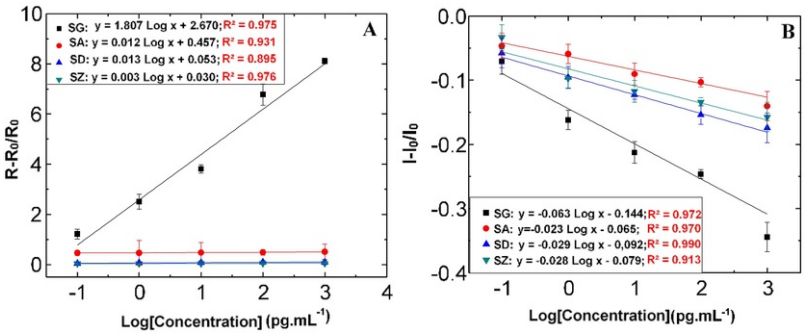

~~Fig. 11.~~Fig. 11 Current and resistance variations of SG, SA, SZ, and SD on imprinted electrodes by using: (A) EIS; (B) DPV, measurements.

alt-text: Fig. 11

~~3.6.~~3.6 Repeatability and stability

The repeatability of the MIP sensor was investigated by measuring each SG concentration three times in the same day on the same device. The relative standard deviation (RSD) of DPV measurements ranged between 1.5% and 8.6%. Therefore, the MIP sensor is expected to be reusable repeatedly. The stability of this system was investigated by monitoring, every day and for seven days, the current response of the concentration 10 pg·mL^{-1} of SG. The results show that the sensor retained 97% of current response after this period, indicating the stability of the prepared sensor over this period.

~~3.7.~~3.7 Recovery study

To evaluate the feasibility of the proposed sensor for detecting SG in real honey samples, a spiked method was performed as follows: 1 g of honey was dissolved in 1 mL of HCl (0.1 M) under magnetic stirring. A dilution ratio of 1:10 (v/v) in PBS (pH 7.4) was employed to reduce the matrix effect, and then filtered through a 0.8 µm cellulose acetate filter. Afterward, the sample was spiked with known amounts of SG standard solutions of SG at two concentrations: 10 pg·mL^{-1} and 100 pg·mL^{-1} and measurements were carried out by DPV and EIS measurements as previously described. The results obtained are shown in Table 2. Satisfactory recoveries of the SG concentration, which ranged between 83.9% and 99.7%, were obtained with good repeatability of $0.8\% < RSD < 3.6\%$ and $5.2\% < RSD < 3.8\%$ for DPV and EIS, respectively. These results indicate that the method reported here is suitable for determining SG in a complex matrix such as honey.

Table 2 Determination of SG in spiked honey samples.

alt-text: Table 2

Methods	Added (pg·mL^{-1})	Found (pg·mL^{-1})	Recovery (%)	RSD (%)
DPV	10.0	9.4	94.0	3.6
	100.0	99.7	99.7	0.8
EIS	10.0	9.2	92.2	5.2
	100.0	83.9	83.9	3.8

~~4.~~4 Conclusion

In the current study, a MIP sensor based on Au-SPE has been successfully developed and applied to detect SG residues in honey samples. This MIP based sensor shows a high recognition capability to SG in comparison to the non-imprinted sensor. Related to the previously reported literature, the developed method displays high sensitivity and selectivity ~~towards~~toward SG against SA, SD, and SZ as interfering molecules. Successful recoveries of 83.9%–99.7% were obtained with an RSD of ~~less than~~ <5.5% in honey samples. In addition, the combination of SG and polyacrylamide results in the high stability of the sensor and the advantages of having good selectivity, accuracy and reproducibility, while keeping low production costs. This would allow its application in the control of food safety. Of greater significance, this approach for achieving a highly sensitive and selective SG electrochemical sensor could be easily extended to the detection of other antibiotics with chemical compatibility with the acrylamide monomer.

Acknowledgements

The project leading to this application has received funding from the European Union's Horizon 2020 research and innovation program under the Marie Skłodowska-Curie grant agreement No 645758, and the financial support of Moulay Ismaïl University under the project of scientific research promotion 2016.

Compliance with ethical standards

Conflict of interest: The author(s) declare that they have no competing interests.

References

[1] G. Font, A. Juan-García and Y. Picó, Pressurized liquid extraction combined with capillary electrophoresis–mass spectrometry as an improved methodology for the determination of sulfonamide residues in meat, ~~J. Chromatogr. A.~~*J. Chromatogr. A* **1159**, 2007, 233–241.

[2] C. Llor and L. Bjerrum, Antimicrobial resistance: risk associated with antibiotic overuse and initiatives to reduce the problem, *Ther. Adv. Drug Saf.* **5**, 2014, 229–241.

[3] S. Bogdanov, Contaminants of bee products, ~~*Apidologic.*~~*Apidologie* **37**, 2006, 1–18.

[4] Ż. Bargańska, J. Namieśnik and M. Ślebioda, Determination of antibiotic residues in honey, *TrAC Trends Anal. Chem.* **30**, 2011, 1035–1041.

[5] A. Ait Lahcen and A. Amine, Mini-review: ~~R~~recent ~~A~~advances in ~~E~~electrochemical ~~D~~determination of ~~S~~sulfonamides, *Anal. Lett.* **51**, 2018, 424–441.

[6] K. Mitrowska and M. Antczak, Determination of sulfonamides in beeswax by liquid chromatography coupled to tandem mass spectrometry, ~~*J. Chromatogr. B.*~~*J. Chromatogr. B* **1006**, 2015, 179–186.

[7] Y.-A. Hammel, R. Mohamed, E. Gremaud, M.-H. LeBreton and P.A. Guy, Multi-screening approach to monitor and quantify 42 antibiotic residues in honey by liquid chromatography–tandem mass spectrometry, ~~J. Chromatogr. A.~~*J. Chromatogr. A* **1177**, 2008, 58–76.

[8] W.M. Mahmoud, N.D. Khaleel, G.M. Hadad, R.A. Abdel-Salam, A. Hai\s s and K. Kümmerer, Simultaneous determination of 11 sulfonamides by HPLC–UV and application for fast screening of their aerobic elimination and biodegradation in a simple test, *Clean: Soil, Air, Water* **41**, 2013, 907–916.

[9] J. Bernal, M.J. Nozal, J.J. Jiménez, M.T. Martín and E. Sanz, A new and simple method to determine trace levels of sulfonamides in honey by high performance liquid chromatography with fluorescence detection, ~~J. Chromatogr. A.~~*J. Chromatogr. A* **1216**, 2009, 7275–7280.

[10] A. Zotou and C. Vasiliadou, LC of sulfonamide residues in poultry muscle and eggs extracts using fluorescence pre-column derivatization and monolithic silica column, *J. Sep. Sci.* **33**, 2010, 11–22.

[11] L. Fotouhi, M. Fatollahzadeh and M.M. Heravi, Electrochemical behavior and voltammetric determination of sulfaguanidine at a glassy carbon electrode modified with a multi-walled carbon nanotube, ~~*Int J Electrochem Sci.*~~*Int. J. Electrochem. Sci.* **7**, 2012, 3919–3928.

[12] A.M. Bueno, A.M. Contento and Á. Ríos, Validation of a screening method for the rapid control of sulfonamide residues based on electrochemical detection using multiwalled carbon nanotubes-glassy carbon electrodes, ~~*Anal. Methods.*~~*Anal. Methods* **5**, 2013, 6821–6829.

[13] T. McGrath, A. Baxter, J. Ferguson, S. Haughey and P. Bjurling, Multi sulfonamide screening in porcine muscle using a surface plasmon resonance biosensor, ~~*Anal. Chim. Acta.*~~*Anal. Chim. Acta* **529**, 2005, 123–127.

[14] G.A. Evtyugin, G.K. Budnikov and A.V. Porfir'eva, Electrochemical DNA-sensors for determining biologically active low-molecular compounds, *Russ. J. Gen. Chem.* **78**, 2008, 2489–2506.

[15] G. Font, M.J. Ruiz, M. Fernández and Y. Picó, Application of capillary electrophoresis-mass spectrometry for determining organic food contaminants and residues, ~~*Electrophoresis.*~~*Electrophoresis* **29**, 2008, 2059–2078.

[16] P. Nagaraja, S. Naik, A. Shrestha and A. Shivakumar, A sensitive spectrophotometric method for the determination of sulfonamides in pharmaceutical preparations, ~~*Acta Pharm.*~~*Acta Pharma.* **57**, 2007, 333–342.

[17] Q. Zhou, D. Peng, Y. Wang, Y. Pan, D. Wan, X. Zhang and Z. Yuan, A novel hapten and monoclonal-based enzyme-linked immunosorbent assay for sulfonamides in edible animal tissues, *Food Chem.* **154**, 2014, 52–62.

[18] N.E.A. El Hassani, S. Motia, B. Bouchikhi and N. El Bari, Synthesis of highly sensitive molecular imprinted sensor for selective determination of doxycycline in honey samples, *World Acad. Sci. Eng. Technol. Int. J. Biol. Biomol. Agric. Food Biotechnol. Eng.* **11**, 2017, 371–374.

[19] ~~N.E.A. El~~N.E.A.E.L. Hassani, A. Baraket, E.T.T. Neto, M. Lee, J.-P. Salvador, M. Marco, J. Bausells, ~~N. El~~N.E.L. Bari, B. Bouchikhi, A. Elaissari, A. Errachid and N. Zine, Novel strategy for sulfapyridine detection using a fully integrated electrochemical Bio-MEMS: ~~A~~application to honey analysis, *Biosens. Bioelectron.* **93**, 2017, 282–288.

[20] M. Bougrini, A. Florea, C. Cristea, R. Sandulescu, F. Vocanson, A. Errachid, B. Bouchikhi, N. El Bari and N. Jaffrezic-Renault, Development of a novel sensitive molecularly imprinted polymer sensor based on electropolymerization of a microporous-metal-organic framework for tetracycline detection in honey, ~~*Food Control.*~~*Food Control* **59**, 2016, 424–429.

[21] L.I. Andersson, Molecular imprinting for drug bioanalysis: a review on the application of imprinted polymers to solid-phase extraction and binding assay, *J. Chromatogr. B Biomed. Sci. Appl.* **739**, 2000, 163–173.

[22] S. Wagner, J. Bell, M. Biyikal, K. Gawlitza and K. Rurack, Integrating fluorescent molecularly imprinted polymer (MIP) sensor particles with a modular microfluidic platform for nanomolar small-molecule detection directly in aqueous samples, *Biosens. Bioelectron.* **99**, 2018, 244–250.

[23] G. Selvolini and G. Marrazza, MIP-based sensors: ~~P~~promising new tools for cancer biomarker determination, ~~*Sensors.*~~*Sensors* **17**, 2017, 718.

[24] J. Ashley, M.-A. Shahbazi, K. Kant, V.A. Chidambara, A. Wolff, D.D. Bang and Y. Sun, Molecularly imprinted polymers for sample preparation and biosensing in food analysis: ~~P~~progress and perspectives, *Biosens. Bioelectron.* **91**, 2017, 606–615.

[25] X. Shi, Y. Meng, J. Liu, A. Sun, D. Li, C. Yao, Y. Lu and J. Chen, Group-selective molecularly imprinted polymer solid-phase extraction for the simultaneous determination of six sulfonamides in aquaculture products, ~~*J. Chromatogr. B.*~~*J. Chromatogr. B* **879**, 2011, 1071–1076.

[26] J. He, S. Wang, G. Fang, H. Zhu and Y. Zhang, Molecularly imprinted polymer online solid-phase extraction coupled with high-performance liquid chromatography-UV for the determination of three sulfonamides in pork and chicken, *J. Agric. Food Chem.* **56**, 2008, 2919–2925.

[27] Y.-G. Zhao, L.-X. Zhou, S.-D. Pan, P.-P. Zhan, X.-H. Chen and M.-C. Jin, Fast determination of 22 sulfonamides from chicken breast muscle using core–shell nanoring amino-functionalized superparamagnetic molecularly imprinted polymer followed by liquid chromatography-tandem mass spectrometry, ~~*J. Chromatogr. A.*~~*J. Chromatogr. A* **1345**, 2014, 17–28.

[28] F.X. Qiao and M.G. Wang, Determination of sulfonamides in milk samples based on RAFT molecularly imprinted solid phase extraction, In: *Adv. Mater. Res.,* 2012, Trans Tech Publ, 1909–1912.

[29] D.M. Pavlović, K. Nikšić, S. Livazović, I. Brnardić and A. Anžlovar, Preparation and application of sulfaguanidine-imprinted polymer on solid-phase extraction of pharmaceuticals from water, ~~*Talanta.*~~*Talanta* **131**, 2015, 99–107.

[30] A. Aldalbahi, M. Rahaman and M. Almoiqli, A ~~S~~strategy to ~~E~~enhance the ~~E~~electrode ~~P~~performance of ~~N~~novel ~~T~~three-~~D~~dimensional PEDOT/RVC ~~C~~composites by ~~E~~electrochemical ~~D~~deposition ~~M~~method, *Polymer* **9**, 2017, 157.

[31] Y. Jin, J. Zhang, W. Zhao, W. Zhang, L. Wang, J. Zhou and Y. Li, Development and validation of a multiclass method for the quantification of veterinary drug residues in honey and royal jelly by liquid chromatography–tandem mass spectrometry, *Food Chem.* **221**, 2017, 1298–1307.

[32] S. Mondal, S.M. Mandal, T.K. Mondal and C. Sinha, Spectroscopic characterization, antimicrobial activity, DFT computation and docking studies of sulfonamide Schiff bases, *J. Mol. Struct.* **1127**, 2017, 557–567.

[33] A. Chandran, H. Tresa Varghese, C. Yohannan Panicker and G. Rajendran, FT-IR and ~~C~~computational ~~S~~study of sulphaguanidine, *Orient. J. Chem.* **27**, 2011, 611.

[34] S.S.A. Abidi, Y. Azim, S.N. Khan and A.U. Khan, Sulfaguanidine cocrystals: ~~S~~synthesis, structural characterization and their antibacterial and hemolytic analysis, *J. Pharm. Biomed. Anal.* **149**, 2018, 351–357.

[35] H. Ji, Y. Wu, Z. Duan, F. Yang, H. Yuan and D. Xiao, Sensitive determination of sulfonamides in environmental water by capillary electrophoresis coupled with both silvering detection window and in-capillary optical fiber light-emitting diode-induced fluorescence detector, ~~*Electrophoresis.*~~*Electrophoresis* **38**, 2017, 452–459.

[36] M.E. Dasenaki, A.A. Bletsou, G.A. Koulis and N.S. Thomaidis, Qualitative multiresidue screening method for 143 veterinary drugs and pharmaceuticals in milk and fish tissue using liquid chromatography quadrupole-time-of-flight mass spectrometry, *J. Agric. Food Chem.* **63**, 2015, 4493–4508.

[37] S. Moretti, G. Cruciani, S. Romanelli, R. Rossi, G. Saluti and R. Galarini, Multiclass method for the determination of 62 antibiotics in milk, *J. Mass Spectrom.* **51**, 2016, 792–804.

[38] M. Franek, I. Diblikova, I. Cernoch, M. Vass and K. Hruska, Broad-specificity immunoassays for sulfonamide detection: immunochemical strategy for generic antibodies and competitors, *Anal. Chem.* **78**, 2006, 1559–1567.

[39] M. Sajid, N. Na, M. Safdar, X. Lu, L. Ma, L. He and J. Ouyang, Rapid trace level determination of sulfonamide residues in honey with online extraction using short C-18 column by high-performance liquid chromatography with fluorescence detection, ~~*J. Chromatogr. A.*~~*J. Chromatogr. A* **1314**, 2013, 173–179.

[40] B. Zhang, Z. Chen, Y. Yu, J. Yang and J. Pan, Determination of sulfonamides in pharmaceuticals and rabbit plasma by microchip electrophoresis with LED-IF detection, ~~*Chromatographia.*~~*Chromatographia* **76**, 2013,

821–829.

Graphical abstract

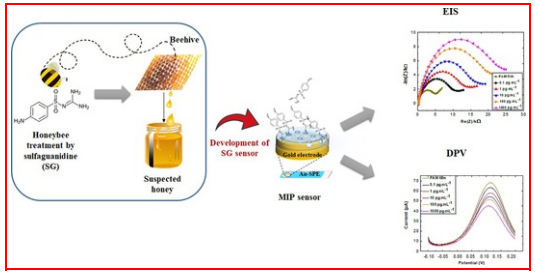

alt-text: Unlabelled Image

Highlights

- Development of electrochemical MIP-based sensor for sulfaguanidine (SG) detection
- The MIP was prepared by electro-polymerization of *acrylamide*.
- Faster synthesis process and great enhancement in the detection limit of SG
- Reducing the time of antibiotic residues analysis in honey samples.
- This system was highly sensitive and selective for SG.

Queries and Answers

Query:

Your article is registered as a regular item and is being processed for inclusion in a regular issue of the journal. If this is NOT correct and your article belongs to a Special Issue/Collection please contact v.gopalsamy@elsevier.com immediately prior to returning your corrections.

Answer: Yes

Query:

Please confirm that given names and surnames have been identified correctly and are presented in the desired order, and please carefully verify the spelling of all authors' names.

Answer: Yes

Query:

The author names have been tagged as given names and surnames (surnames are highlighted in teal color). Please confirm if they have been identified correctly.

Answer: The last name of the first author is all: **El Alami El Hassani**

Query:

Please confirm that the provided email n_elbari@hotmail.com is the correct address for official communication, else provide an alternate e-mail address to replace the existing one, because private e-mail addresses should not be used in articles as the address for communication.

Answer: I confirm the corresponding email: n_elbari@hotmail.com

Query:

Please provide the corresponding grant number(s) for the following grant sponsor(s): "Moulay Ismaïl University".

Answer: "European Union's Horizon 2020 research and innovation program under the Marie Skłodowska-Curie grant agreement **No 645758"**